Surface Science Spectra

RESEARCH ARTICLE | NOVEMBER 16 2023

XPS study of NiO thin films obtained by chemical vapor deposition

Special Collection: Materials for Energy and the Environment

Gioele Pagot ; Mattia Benedet ; Chiara Maccato ; Davide Barreca ; Vito Di Noto

Check for updates

Surf. Sci. Spectra 30, 024028 (2023)
https://doi.org/10.1116/6.0003008

View Online
Export Citation

Articles You May Be Interested In

Propargyl carbamate-functionalized Cu(II)-metal organic framework after reaction with chloroauric acid: An x-ray photoelectron spectroscopy data record

Surf. Sci. Spectra (September 2022)

XPS investigation of F-doped MnO_2 nanosystems fabricated by plasma assisted-CVD

Surf. Sci. Spectra (December 2018)

13 January 2025 13:14:18

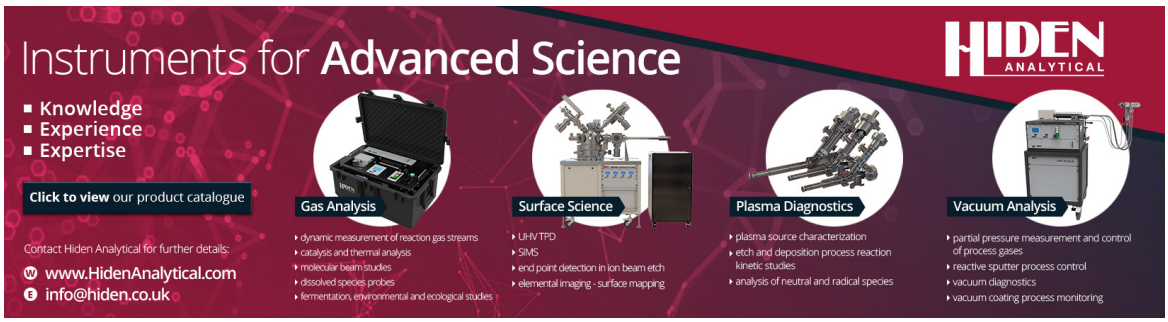

SSS SURFACE SCIENCE SPECTRA

ARTICLE

pubs.aip.org/avs/sss

XPS study of NiO thin films obtained by chemical vapor deposition

Cite as: Surf. Sci. Spectra 30, 024028 (2023); doi: 10.1116/6.0003008
Submitted: 27 July 2023 · Accepted: 26 September 2023 ·
Published Online: 16 November 2023

View Online Export Citation CrossMark

Gioele Pagot,[1] Mattia Benedet,[2,3] Chiara Maccato,[2,3] Davide Barreca,[3] and Vito Di Noto[1,a)]

AFFILIATIONS

[1]Section of Chemistry for the Technology (ChemTech) and INSTM, Department of Industrial Engineering, University of Padova, Via Marzolo 9, I-35131 Padova (PD), Italy
[2]Department of Chemical Sciences, Padova University and INSTM, Via Marzolo 1, I-35131 Padova (PD), Italy
[3]CNR-ICMATE and INSTM, Department of Chemical Sciences, Padova University, Via Marzolo 1, I-35131 Padova, Italy

Note: This paper is part of the 2023 Special Topic Collection on Materials for Energy and the Environment.
[a)]**Author to whom correspondence should be addressed:** vito.dinoto@unipd.it

ABSTRACT

Nickel oxide (NiO) thin films are of great importance for a variety of technological applications, especially in (photo)electrocatalysis for clean energy production and pollutant degradation. In this field, various research efforts are devoted to the preparation of thin films with controllable chemicophysical properties. In the framework of our research activities, we have recently fabricated NiO thin films by means of chemical vapor deposition (CVD) using a series of closely related Ni(II) β-diketonate-diamine molecular precursors. In the present work, the attention is focused on the x-ray photoelectron spectroscopy (XPS) analysis of a representative NiO film grown at 400 °C in an $O_2 + H_2O$ reaction atmosphere. Besides the wide scan spectrum, high resolution spectra for C 1*s*, O 1*s*, and, in particular, Ni 2*p* are reported and discussed in detail.

Key words: NiO, thin films, chemical vapor deposition, x-ray photoelectron spectroscopy

© 2023 Author(s). All article content, except where otherwise noted, is licensed under a Creative Commons Attribution (CC BY) license (http://creativecommons.org/licenses/by/4.0/). https://doi.org/10.1116/6.0003008

13 January 2025 13:14:18

Accession#: 01869
Technique: XPS
Specimen: NiO
Instrument: SPECS EnviroESCA
Major Elements in Spectra: C, O, and Ni
Minor Elements in Spectra: None
Published Spectra: 4
Spectral Category: Comparison

INTRODUCTION

Nickel oxide (NiO) thin films have gained significant attention in recent years due to their attractive photocatalytic and electrocatalytic properties (Refs. 1–4). These systems exhibit a unique combination of semiconducting behavior and excellent stability, making them promising candidates for various applications, particularly in the fields of energy conversion and environmental remediation. As photocatalysts, NiO thin films have shown great potential in harnessing solar energy for water splitting, pollutant degradation, and CO_2 reduction, offering a sustainable approach to address the global energy and environmental challenges. The bandgap of NiO thin films can be engineered by controlling their thickness and doping, allowing for efficient utilization of a broader solar spetrum range (Ref. 5). Furthermore, surface modification techniques such as metal cocatalyst deposition and nanoparticle loading have been explored to enhance the photocatalytic activity and charge separation efficiency of NiO thin films. As electrocatalysts, the latter have demonstrated remarkable performances in electrochemical water splitting systems, for the oxygen evolution reaction, and energy storage devices, such as supercapacitors. Their high electrochemical stability, excellent charge transport properties, and abundant active sites contribute to their outstanding catalytic performances. In this regard, advances in synthetic techniques, including atomic layer deposition, sol-gel methods, and electrodeposition, have enabled

© Author(s) 2023

precise control over the composition, morphology, and nanostructuring of NiO thin films, enabling to boost and tailor their functional activity as a function of the specific end-use (Ref. 6).

In the framework of our recent research projects, we have dedicated various efforts to chemical vapor deposition (CVD) of NiO films from diketonate-diamine adducts. In this study, we present and discuss the outcomes of an XPS investigation on a representative specimen performed using an Al K_α x-ray source, analyzing the C 1*s*, O 1*s*, and Ni 2*p* spectral regions.

SPECIMEN DESCRIPTION (ACCESSION # 01869)

Specimen: NiO thin film supported on Si(100)
CAS Registry #: 1313-99-1
Specimen Characteristics: Homogeneous; solid; polycrystalline; semiconductor; inorganic compound; thin film
Chemical Name: Nickel(II) oxide
Source: Sample deposited on Si(100) by CVD
Composition: C, O, and Ni
Form: Supported thin film
Structure: The film x-ray diffraction (XRD) pattern displayed two signals due to (111) and (200) crystallographic planes of cubic NiO ($2\theta = 37.2°$ and 43.3°, respectively) (Ref. 7). A comparison of the actual relative intensities with the ones of the reference patter highlighted the occurrence of a (100) preferential orientation. The average crystallite dimensions were estimated to be 18 nm by means of the Scherrer formula. Scanning electron microscopy (SEM) analyses revealed the formation of a columnar-type film uniformly covering the substrate surface, with a mean thickness of 170 nm.
History and Significance: A cold-wall, horizontal custom-built apparatus, equipped with a resistively heated metal susceptor and a quartz chamber, was used for the CVD of NiO thin films. In a typical deposition experiment, the $Ni(dpm)_2TMEDA$ precursor (Hdpm = 2,2,6,6-tetramethyl-3,5-heptanedione, TMEDA = *N*,*N*,*N*′,*N*′-tetramethylethylenediamine), synthesized as previously reported (Ref. 6), was heated in a glass vaporizer at 120 °C by means of an external oil bath, and its vapors were delivered into the reactor chamber by means of an electronic grade O_2 flow [100 standard cubic centimeters per minute (SCCM)]. The gas lines connecting the precursor vessel and the reaction chamber were heated at 140 °C by means of external tapes to avoid detrimental precursor condensation. An additional electronic grade oxygen flow (100 SCCM) was separately introduced into the reactor after passing through a water reservoir maintained at 35 °C. Growth processes were carried out at a total pressure of 10.0 mbar and a temperature of 400 °C on Si(100) substrates (MEMC Electronic Materials S.p.A, Merano (BZ), Italy), precleaned by sonication in isopropylic alcohol, dichloroethane, and final etching in a 2% HF solution.
As Received Condition: As grown
Analyzed Region: Same as the host material
***Ex Situ* Preparation/Mounting:** Sample crimped on a metal stub accessory and introduced into the analysis chamber.
***In Situ* Preparation:** None
Charge Control: No flood gun was used during the analysis. For further details on the charging correction procedure, see Data Analysis Methods, Energy Scale Correction.
Temp. During Analysis: 298 K
Pressure During Analysis: $<1 \times 10^{-4}$ Pa
Preanalysis Beam Exposure: 180 s

INSTRUMENT DESCRIPTION

Manufacturer and Model: SPECS EnviroESCA
Analyzer Type: Spherical sector
Detector: Other 1D delay line detector (1D-DLD)
Number of Detector Elements: 25

INSTRUMENT PARAMETERS COMMON TO ALL SPECTRA

Spectrometer

Analyzer Mode: Constant pass energy
Throughput ($T = E^N$): N = 0
Excitation Source Window: Silicon nitride
Excitation Source: Al K_α monochromatic
Source Energy: 1486.6 eV
Source Strength: 56 W
Source Beam Size: $250 \times 250\ \mu m^2$
Signal Mode: Multichannel direct

Geometry

Incident Angle: 55°
Source-to-Analyzer Angle: 55°
Emission Angle: 0°
Specimen Azimuthal Angle: 0°
Acceptance Angle from Analyzer Axis: 22°
Analyzer Angular Acceptance Width: 44°

13 January 2025 13:14:18

DATA ANALYSIS METHOD

Energy Scale Correction: Binding energy (BE) values were corrected for charging by assigning to the adventitious C 1*s* peak a BE of 284.8 eV (Ref. 8).
Recommended Energy Scale Shift: −0.042 eV
Peak Shape and Background Method: Gaussian–Lorentzian sum functions with a Shirley background were used for peak fitting.
Quantitation Method: Atomic concentrations were calculated by peak area integration using sensitivity factors provided by SPECS software (SpecsLab Prodigy Version 4.94.2).

ACKNOWLEDGMENTS

G.P. and V.D.N. gratefully acknowledge the Padova University for support via the program "Budget Integrato per la Ricerca Interdipartimentale—BIRD 2021" under Project No. BIRD219831. Financial support from the National Council of Research (Progetti di Ricerca @CNR—avviso 2020—ASSIST), Padova University (Department of Chemical Sciences, DOR 2021-2023, P-DiSC#04BIRD2020-UNIPD EUREKA), and INSTM Consortium (INSTM21PDBARMAC-ATENA) is also gratefully acknowledged.

© Author(s) 2023

Thanks are also due to Dr. Davide Canton for experimental support and to Prof. Mauro Sambi for helpful discussions.

AUTHOR DECLARATIONS

Conflict of Interest

The authors have no conflicts to disclose.

Author Contributions

Gioele Pagot: Funding acquisition (equal); Investigation (equal); Writing – original draft (equal); Writing – review & editing (equal). **Mattia Benedet:** Investigation (equal); Writing – original draft (equal); Writing – review & editing (equal). **Chiara Maccato:** Conceptualization (equal); Funding acquisition (equal); Supervision (equal); Writing – review & editing (equal). **Davide Barreca:** Conceptualization (equal); Funding acquisition (equal); Writing – original draft (equal); Writing – review & editing (equal). **Vito Di Noto:** Conceptualization (equal); Funding acquisition (equal); Supervision (equal); Writing – original draft (equal); Writing – review & editing (equal).

DATA AVAILABILITY

The data that support the findings of this study are available within the article and its supplementary material.

REFERENCES

[1]N. Spinner and W. E. Mustain, Electrochim. Acta **56**, 5656 (2011).
[2]M. Gong *et al.*, Nat. Commun. **5**, 4695 (2014).
[3]A. Akbari, Z. Sabouri, H. A. Hosseini, A. Hashemzadeh, M. Khatami, and M. Darroudi, Inorg. Chem. Comm. **115**, 107867 (2020).
[4]C. Hu, K. Chu, Y. Zhao, and W. Y. Teoh, ACS Appl. Mater. Interfaces **6**, 18558 (2014).
[5]A. Mallikarjuna Reddy, A. Sivasankar Reddy, and P. Sreedhara Reddy, Vacuum **85**, 949 (2011).
[6]M. Benedet *et al.*, Dalton Trans. **52**, 10677 (2023).
[7]Pattern No. 00-0047-1049, JCPDS (2000).
[8]D. Briggs and M. P. Seah, *Practical Surface Analysis: Auger and X-Ray Photoelectron Spectroscopy*, 2nd ed. (John Wiley & Sons, New York, 1990), pp. 1–657.
[9]L. Bigiani, D. Barreca, A. Gasparotto, and C. Maccato, Surf. Sci. Spectra **25**, 014003 (2018).
[10]J. F. Moulder, W. F. Stickle, P. E. Sobol, and K. D. Bomben, *Handbook of X-Ray Photoelectron Spectroscopy* (Perkin Elmer Corporation, Eden Prairie, MN, 1992), p. 55344.
[11]N. Weidler, J. Schuch, F. Knaus, P. Stenner, S. Hoch, A. Maljusch, R. Schäfer, B. Kaiser, and W. Jaegermann, J. Phys. Chem. C **121**, 6455 (2017).
[12]D. Alders, F. C. Voogt, T. Hibma, and G. A. Sawatzky, Phys. Rev. B **54**, 7716 (1996).
[13]S. Altieri, L. H. Tjeng, A. Tanaka, and G. A. Sawatzky, Phys. Rev. B **61**, 13403 (2000).
[14]D. S. Kim and H. C. Lee, J. Appl. Phys. **112**, 034504 (2012).
[15]P. Salunkhe, M. Ali A V, and D. Kekuda, Mater. Res. Express **7**, 016427 (2020).
[16]M. Basato, E. Faggin, C. Tubaro, and A. C. Veronese, Polyhedron **28**, 1229 (2009).
[17]R. L. Wilson *et al.*, RSC Adv. **11**, 22199 (2021).
[18]Y. Zhang, L. Du, X. Liu, and Y. Ding, Appl. Surf. Sci. **481**, 138 (2019).
[19]M. C. Biesinger, B. P. Payne, L. W. M. Lau, A. Gerson, and R. S. C. Smart, Surf. Interf. Analysis **41**, 324 (2009).
[20]D. Barreca *et al.*, J. Phys. Chem. C **122**, 1367 (2018).
[21]G. Carraro, D. Barreca, D. Bekermann, T. Montini, A. Gasparotto, V. Gombac, C. Maccato, and P. Fornasiero, J. Nanosci. Nanotechnol. **13**, 4962 (2013).
[22]L. Bigiani, D. Barreca, A. Gasparotto, C. Sada, S. Martí-Sanchez, J. Arbiol, and C. Maccato, CrystEngComm **20**, 3016 (2018).
[23]L. Armelao, D. Barreca, S. Gross, and E. Tondello, Surf. Sci. Spectra **8**, 14 (2001).
[24]See http://srdata.nist.gov/xps.
[25]H. W. Nesbitt, D. Legrand, and G. M. Bancroft, Phys. Chem. Minerals **27**, 357 (2000).
[26]S. D'Addato, V. Grillo, S. Altieri, R. Tondi, S. Valeri, and S. Frabboni, J. Phys.: Condens. Matter **23**, 175003 (2011).
[27]M. C. Biesinger, L. W. M. Lau, A. R. Gerson, and R. S. C. Smart, Phys. Chem. Chem. Phys. **14**, 2434 (2012).
[28]C. Stienen, J. Grahl, C. Wölper, S. Schulz, and G. Bendt, RSC Adv. **12**, 22974 (2022).
[29]K. C. Min *et al.*, Surf. Coat. Technol. **201**, 9252 (2007).
[30]A. N. Mansour, Surf. Sci. Spectra **3**, 231 (1994).
[31]J. Tian, H. Jiang, X. Zhao, G. Shi, Y. Dai, X. Deng, H. Xie, and W. Zhang, Sens. Actuators B Chem. **366**, 131981 (2022).
[32]N. Kitchamsetti, M. S. Ramteke, S. R. Rondiya, S. R. Mulani, M. S. Patil, R. W. Cross, N. Y. Dzade, and R. S. Devan, J. Alloys Compds **855**, 157337 (2021).
[33]A. Kotta, E.-B. Kim, S. Ameen, H.-S. Shin, and H. K. Seo, J. Electrochem. Soc. **167**, 167517 (2020).
[34]D. Zywitzki, D. H. Taffa, L. Lamkowski, M. Winter, D. Rogalla, M. Wark, and A. Devi, Inorg. Chem. **59**, 10059 (2020).
[35]X. Geng, D. Lahem, C. Zhang, C.-J. Li, M.-G. Olivier, and M. Debliquy, Ceram. Int. **45**, 4253 (2019).
[36]P. Dubey, N. Kaurav, R. S. Devan, G. S. Okram, and Y. K. Kuo, RSC Adv. **8**, 5882 (2018).
[37]W.-c. Yeh and M. Matsumura, Jpn. J. Appl. Phys. **36**, 6884 (1997).
[38]S. W. Han, I. H. Kim, D. H. Kim, K. J. Park, E. J. Park, M.-G. Jeong, and Y. D. Kim, Appl. Surf. Sci. **385**, 597 (2016).
[39]J.-K. Kang and S.-W. Rhee, Thin Solid Films **391**, 57 (2001).
[40]A. S. Kondrateva, M. Mishin, A. Shakhmin, M. Baryshnikova, and S. E. Alexandrov, Phys. Status Solidi C **12**, 912 (2015).
[41]T. S. Yang, W. Cho, M. Kim, K.-S. An, T.-M. Chung, C. G. Kim, and Y. Kim, J. Vac. Sci. Technol. A **23**, 1238 (2005).

13 January 2025 13:14:18

© Author(s) 2023

SPECTRAL FEATURES TABLE

Spectrum ID #	Element/ Transition	Peak Energy (eV)	Peak Width FWHM (eV)	Peak Area (eV x cts)	Sensitivity Factor	Concentration (at. %)	Peak Assignment
01869-02[a]	C 1*s*	284.8	1.3	4593.6	1	29.0	Adventitious surface contamination
01869-02[a]	C 1*s*	286.4	1.3	510.6	1	3.2	C–O species from precursor residuals
01869-02[a]	C 1*s*	288.3	1.3	490.7	1	3.1	Chemisorbed carbonates
01869-03[b]	O 1*s*	529.9	1.3	7236.1	2.48	18.4	Lattice oxygen in NiO
01869-03[b]	O 1*s*	531.5	1.8	5833.2	2.48	14.9	Surface-chemisorbed hydroxyls/carbonates
01869-03[b]	O 1*s*	533.0	1.8	968.5	2.48	2.5	Adsorbed water
01869-04[c]	Ni 2*p*	…	…	74 074.1	16.18	28.9	…
01869-04[d]	Ni $2p_{3/2}$	853.8	…	…	…	…	NiO (**1**)
01869-04[d]	Ni $2p_{3/2}$	855.3	…	…	…	…	NiO (**2**)
01869-04[d]	Ni $2p_{1/2}$	860.7	…	…	…	…	NiO (**3**)
01869-04[d,e]	Ni $2p_{1/2}$	872.0	…	…	…	…	NiO (**4**,**5**)
01869-04[d]	Ni $2p_{1/2}$	879.4	…	…	…	…	NiO (**6**)

Comment to Spectral Features Table:

[a]The sensitivity factor is referred to the whole C 1*s* signal.

[b]The sensitivity factor is referred to the whole O 1*s* signal.

[c]The sensitivity factor, peak area, and concentration are referred to the whole Ni 2*p* signal.

[d]For the attribution of spectral features **1**–**6**, refer to **Footnote to Spectrum 01869-04**.

[e]Components (**4**) and (**5**) are partially overlapped and give rise to the band located at 872.0 eV.

Footnote to Spectrum 01869-02: The C 1*s* signal was characterized by the presence of three contributing bands. The most intense one (82.1% of the total carbon amount), located at BE = 284.8 eV, was related to adventitious contamination arising from air exposure and sample manipulation prior to the analysis. The band centered at BE = 286.4 eV, corresponding to 9.1% of the total carbon content, was related to C–O species from Ni precursor residuals, whereas the peak at BE = 288.3 eV was due to the presence of chemisorbed carbonates (Refs. 8–11). This assignment is in line with O 1*s* peak fitting results (see comments to Spectrum 01869-03).

Footnote to Spectrum 01869-03: Three components contributed to the O 1*s* signal. The one centered at a BE of 529.9 eV (≈50.0% of the total oxygen) was due to lattice oxygen in the NiO network (Refs. 12–18), whereas the band at BE = 531.5 eV was ascribed to the presence of both hydroxyl and C–O moieties, such as chemisorbed carbonates (Refs. 9–11 and 19–22). The third band, centered at 533.0 eV, was due to adsorbed H_2O (Refs. 10, 23, and 24). The presence of the latter two bands, arising from the use of water vapor as coreactant during the growth process, was responsible for a O/Ni atomic percentage ratio slightly higher than the stoichiometric value.

Footnote to Spectrum 01869-04: The Ni 2*p* photopeak, featuring a shape and energy position in agreement with previous data for NiO (Refs. 10, 12, 13, 19, and 25–30), displays a much more complex profile than the simple doublet expected on the basis of the sole spin–orbit splitting. In figure 01869-04, **1**, **2,** and **3** labels (located at 853.8, 855.3, and 860.7 eV, respectively) refer to the $2p_{3/2}$ spin–orbit split component features, whereas **4** and **5** (partially overlapped, yielding the feature at 872.0 eV) and **6** (at 879.4 eV) labels mark the $2p_{1/2}$ ones. The correct assignment of these features is still controversial, and indeed contrasting interpretations are available in the literature so far. In different works, the doubly peaked main line was related to the occurrence of Ni(III) centers at the system surface (Refs. 14, 15, and 31–38), and in various cases, Ni(III) contents comparable, or even higher, than Ni(II) ones (Refs. 31, 33, 35, and 36), or the formation of a Ni_2O_3 subsidiary phase along with NiO (Refs. 15, 32, 37, and 39–41) has been claimed basing on the sole XPS data. Nonetheless, this interpretation contradicts not only experimental results obtained by x-ray absorption spectroscopy (XAS), but also the presence of the same spectral features even for NiO single crystals freshly cleaved in vacuum, indicating that the target satellite structure is unique to NiO (Refs. 12 and 13). Hence, a realistic understanding of Ni 2*p* signal shape should not take into account variations in the metal center oxidation state, but rather a contribution of the coordinated O electronic states to Ni 2*p* spectral features (Ref. 25).

One of the explanations proposed for the overall Ni 2*p* signal shape in NiO, with a $3d^8$ configuration of metal centers, is as follows. The formation of a hole in the Ni2p core level upon photoionization is accompanied by a strong Coulomb repulsion with the holes present in 3*d* orbitals. Although the ground state features a predominant $3d^8$ character, the lowest energy will be corresponding to a $\underline{\boldsymbol{c}}3d^9\underline{\boldsymbol{O}}$ state [**1** and **4** peaks (Ref. 26)], where $\underline{\boldsymbol{c}}$ and $\underline{\boldsymbol{O}}$ indicate a hole in the 2*p* core level and the O band, respectively. **3** and **6** structures, which have generally been regarded as "shake-off" satellites, can be attributed to unscreened $\underline{\boldsymbol{c}}3d^8$ final states (Ref. 26). Nonetheless, this model does not provide an explanation for features **2** and **5**. In this regard, a valuable explanation was proposed by Sawatzky *et al.*, who argued that the 2*p* core-level line shape is significantly affected not only by nearest-neighbors, but also by next-nearest-neighbor configurations (Ref. 12). According to this *nonlocal* screening mechanism, which involves at least two sites, a core hole can also be screened by an electron coming from a neighboring NiO_6 unit and not necessarily from O atoms bonded to the emitting Ni site. The validity of this *nonlocal* screening process is highlighted by the fact that even inclusion of multiplet effects cannot reproduce the Ni 2*p* NiO spectrum if one uses a single-Ni-site model (Ref. 13). The *nonlocal* screening process accounts for a general consensus on the assignment of the above features. The satellite intensity is directly dependent on the local environment and is hence very sensitive to material crystallinity and defectivity (Ref. 12).

On the basis of the above observations, **2** and **5** features originate from screening by an electron that does not come from O orbitals around the Ni(II) center bearing the core hole but from an adjacent NiO_6 unit. In particular, after the creation of a core hole ($3d^8 \rightarrow \underline{\boldsymbol{c}}3d^8$), the system energy can be lowered thanks to screening electrons from neighboring sites, yielding $\underline{\boldsymbol{c}}3d^8 \rightarrow \underline{\boldsymbol{c}}3d^9\underline{\boldsymbol{O}}$ states. According to the *nonlocal* screening mechanism, an electron is transferred from a neighboring NiO_6 unit: $\underline{\boldsymbol{c}}3d^8$; $3d^8 \rightarrow \underline{\boldsymbol{c}}3d^9;3d^8\underline{\boldsymbol{O}}$. This yields a main $2p^53d^9$ character for the local configuration at the emitting Ni site (Ref. 13) and an extra-hole $3d^8\underline{\boldsymbol{O}}$ in a neighboring unit (Ref. 12).

In spite of this explanation, it is worthwhile noticing that the matter is still subject of debate, since quantum chemical calculations on NiO using a variety of approaches suggest a Ni ground state charge lower than 2, and, in particular, ranging from 1.33 to 1.68, as resulting from density functional calculations. In line with this interpretation, in the ground state, no $\underline{\boldsymbol{c}}$ is present and the initial state electron configuration is better written as $3d^{8+\delta}\underline{\boldsymbol{O}}^{-\delta}$ (Ref. 27).

13 January 2025 13:14:18

© Author(s) 2023

ANALYZER CALIBRATION TABLE

Spectrum ID #	Element/ Transition	Peak Energy (eV)	Peak Width FWHM (eV)	Peak Area (eV x cts)	Sensitivity Factor	Concentration (at. %)	Peak Assignment
…[a]	Ag $3d_{5/2}$	368.2	0.7	73 229.4	…	…	Ag(0)

[a]The peak was acquired after Ar^+ erosion.

13 January 2025 13:14:18

GUIDE TO FIGURES

Spectrum (Accession) #	Spectral Region	Voltage Shift[a]	Multiplier	Baseline	Comment #
01869-01	Survey	+0.042	1	0	…
01869-02	C 1*s*	+0.042	1	0	…
01869-03	O 1*s*	+0.042	1	0	…
01869-04	Ni 2*p*	+0.042	1	0	…

[a]Voltage shift of the archived (as-measured) spectrum relative to the printed figure. The figure reflects the recommended energy scale correction due to a calibration correction, sample charging, flood gun, or other phenomenon.

© Author(s) 2023

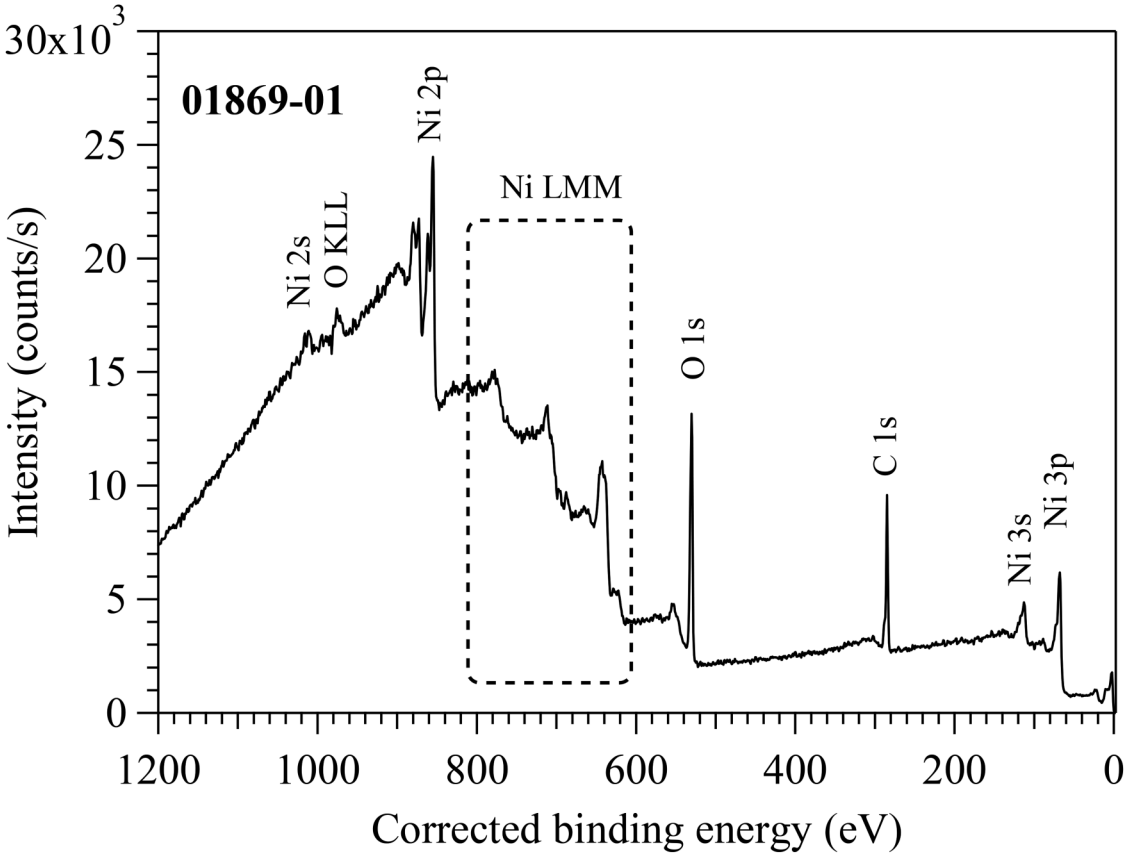

13 January 2025 13:14:18

Accession #	01869-01
■ Specimen	NiO
■ Technique	XPS
■ Spectral Region	Survey
Instrument	SPECS EnviroESCA
Excitation Source	Al K_α monochromatic
Source Energy	1486.6 eV
Source Strength	56 W
Source Size	0.250 × 0.250 mm^2
Analyzer Type	Spherical sector analyzer
Incident Angle	55°
Emission Angle	0°
Analyzer Pass Energy	100 eV
Analyzer Resolution	1.0 eV
Total Signal Accumulation Time	651.6 s
Total Elapsed Time	844.0 s
Number of Scans	2
Effective Detector Width	1.0 eV

© Author(s) 2023

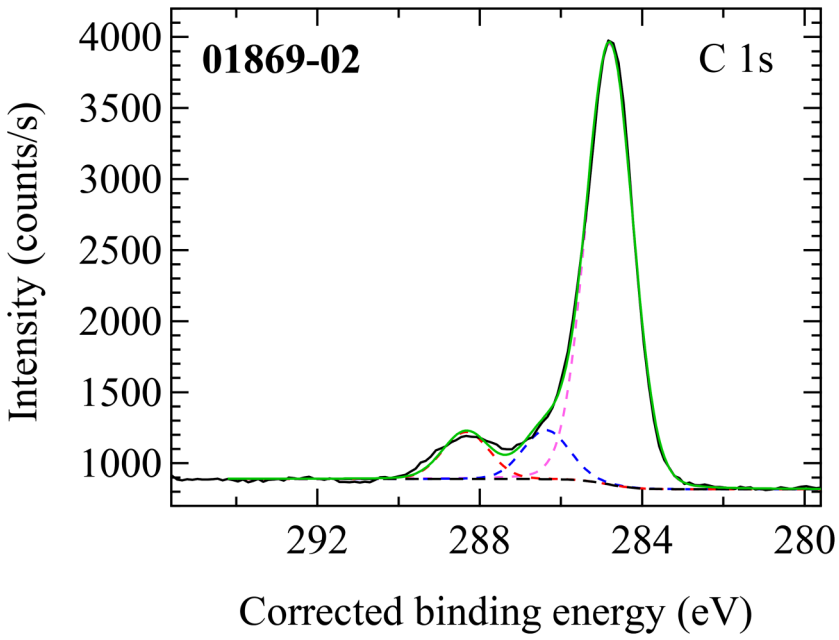

- **Accession #:** 01869-02
- **Specimen:** NiO
- **Technique:** XPS
- **Spectral Region:** C 1*s*

Instrument: SPECS EnviroESCA
Excitation Source: Al K_α monochromatic
Source Energy: 1486.6 eV
Source Strength: 56 W
Source Size: 0.250 × 0.250 mm^2
Analyzer Type: Spherical sector
Incident Angle: 55°
Emission Angle: 0°
Analyzer Pass Energy: 40 eV
Analyzer Resolution: 0.4 eV
Total Signal Accumulation Time: 1387.5 s
Total Elapsed Time: 1982.5 s
Number of Scans: 15
Effective Detector Width: 0.4 eV

13 January 2025 13:14:18

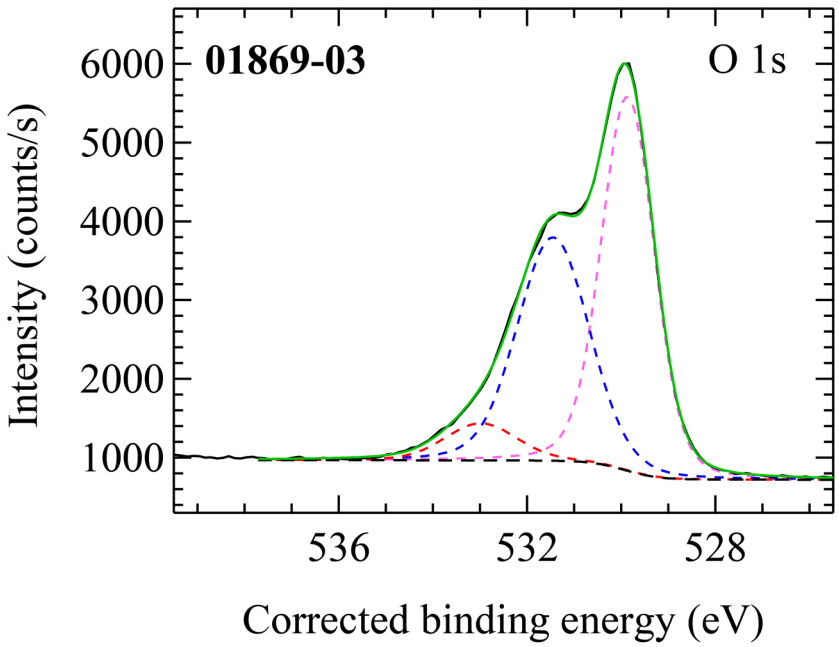

- **Accession #:** 01869-03
- **Specimen:** NiO
- **Technique:** XPS
- **Spectral Region:** O 1*s*

Instrument: SPECS EnviroESCA
Excitation Source: Al K_α monochromatic
Source Energy: 1486.6 eV
Source Strength: 56 W
Source Size: 0.250 × 0.250 mm^2
Analyzer Type: Spherical sector
Incident Angle: 55°
Emission Angle: 0°
Analyzer Pass Energy: 40 eV
Analyzer Resolution: 0.4 eV
Total Signal Accumulation Time: 1327.5 s
Total Elapsed Time: 1896.0 s
Number of Scans: 15
Effective Detector Width: 0.4 eV

© Author(s) 2023

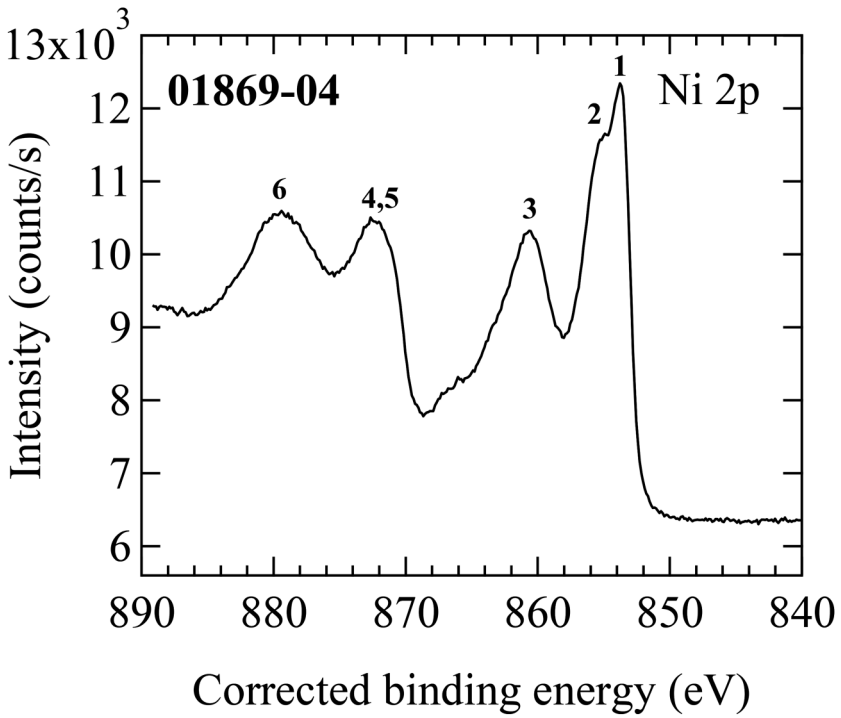

- **Accession #:** 01869-04
- **Specimen:** NiO
- **Technique:** XPS
- **Spectral Region:** Ni 2*p*

Instrument: SPECS EnviroESCA
Excitation Source: Al K_α monochromatic
Source Energy: 1486.6 eV
Source Strength: 56 W
Source Size: 0.250 × 0.250 mm^2
Analyzer Type: Spherical sector
Incident Angle: 55°
Emission Angle: 0°
Analyzer Pass Energy: 40 eV
Analyzer Resolution: 0.4 eV
Total Signal Accumulation Time: 5012.5 s
Total Elapsed Time: 7159.0 s
Number of Scans: 25
Effective Detector Width: 0.4 eV

13 January 2025 13:14:18

© Author(s) 2023